

## On the Neutrino Flux from Gamma-Ray Bursts

D. Guetta<sup>1</sup>, M. Spada<sup>1</sup>, E. Waxman<sup>2</sup>

### ABSTRACT

Observations imply that gamma-ray bursts (GRBs) are produced by the dissipation of the kinetic energy of a highly relativistic fireball. Photo-meson interactions of protons with  $\gamma$ -rays within the fireball dissipation region are expected to convert a significant fraction of fireball energy to  $> 10^{14}$  eV neutrinos. We present an analysis of the internal shock model of GRBs, where production of synchrotron photons and photo-meson neutrinos are self-consistently calculated, and show that the fraction of fireball energy converted to high energy neutrinos is not sensitive to uncertainties in fireball model parameters, such as the expansion Lorentz factor and characteristic variability time. This is due in part to the constraints imposed on fireball parameters by observed GRB characteristics, and in part to the fact that for parameter values for which the photo-meson optical depth is high (implying high proton energy loss to pion production) neutrino production is suppressed by pion and muon synchrotron losses. The neutrino flux is therefore expected to be correlated mainly with the observed  $\gamma$ -ray flux. The time averaged neutrino intensity predicted by the model,  $\sim 10^{-8.5}$  GeV/cm<sup>2</sup>sr, is consistent with the flux predicted by the assumption that GRBs are the sources of  $> 10^{19}$  eV cosmic-rays.

*Subject headings:* gamma-rays: bursts–elementary particles–acceleration of particles–methods: numerical

### 1. INTRODUCTION

The characteristics of  $\gamma$ -ray bursts (GRBs), bursts of 0.1 MeV–1 MeV photons lasting for a few seconds (Fishman & Meegan 1995), suggest that the observed radiation is produced by the dissipation of the kinetic energy of a relativistically expanding wind, a “fireball,” at cosmological distance (see, e.g., Piran 1999 for review). The recent detection of delayed low energy (X-ray to radio) emission (afterglow) from GRB sources (see Kulkarni *et al.* 2000 for review), confirmed

---

<sup>1</sup>Osservatorio di Arcetri Largo E. Fermi 5, 50125 Firenze, Italy

<sup>2</sup>Department of Condensed Matter Physics, Weizmann Institute, Rehovot 76100, Israel

both the cosmological origin of the bursts and standard model predictions of afterglows, that result from the collision of an expanding fireball with its surrounding medium (see Mészáros 1999 for review).

Within the fireball model framework, observed  $\gamma$ -rays are produced by synchrotron emission of electrons accelerated to high energy by internal shocks within the expanding wind. In the region where electrons are accelerated, protons are also expected to be shock accelerated: Plasma parameters in the dissipation region allow proton acceleration to  $> 10^{20}$  eV (Waxman 1995a, Vietri 1995; see Waxman 2000 for a recent review). A natural consequence of proton acceleration to high energy is the production of a burst of  $\gtrsim 10^{14}$  eV neutrinos (Waxman & Bahcall 1997,2000), produced by the decay of charged pions created in interactions between fireball photons and high energy protons. Lower energy neutrinos may be produced by inelastic nuclear collisions (Bahcall & Mészáros 2000, Mészáros & Rees 2000).

The characteristic energy of neutrinos produced by photo-meson interactions is determined by the relation between the observed photon energy,  $E_\gamma$ , and the accelerated proton’s energy,  $E_p$ , at the photo-meson threshold of the  $\Delta$ -resonance. In the observer frame,

$$E_\gamma E_p = 0.2 \text{ GeV}^2 \Gamma^2, \quad (1)$$

where phenomenologically the Lorentz factors of the expanding fireball are  $\Gamma > 10^2$ . For typical observed  $\gamma$ -ray energy of 1 MeV, proton energies  $E_p \approx 2 \times 10^7$  GeV are required to produce neutrinos from pion decay, leading to  $\approx 10^{15}$  eV neutrinos. Both  $\sim 1$  MeV photons and  $\sim 10^{15}$  eV neutrinos are produced in this model during the stage of internal shocks within the expanding wind. Much higher energy,  $\gtrsim 10^{18}$  eV, neutrinos may be produced at a later stage, at the onset of fireball interaction with its surrounding medium. Optical–UV photons are radiated by electrons accelerated in shocks propagating backward into the fireball plasma. Protons are accelerated to high energy in these “reverse” shocks. The combination of low energy photons and high energy protons produces ultra-high energy neutrinos via photo-meson interactions, as indicated by Eq. (1).

The predicted flux of  $\gtrsim 10^{14}$  eV neutrinos produced in internal shocks is determined by the fraction  $f_\pi$  of fireball proton energy lost to pion production. This fraction is determined by the number density of photons at the internal dissipation region, and is given by (Waxman & Bahcall 1997,1999)

$$f_\pi(E_p) \approx 0.2 \min(1, E_p/E_p^b) \frac{L_{\gamma,52}}{\Gamma_{2.5}^4 \Delta t_{-2} E_{\gamma,\text{MeV}}^b}. \quad (2)$$

The  $\gamma$ -ray luminosity  $L_\gamma$ , the photon spectral break energy  $E_\gamma^b$  (where luminosity per logarithmic photon energy interval peaks), the observed variability time  $\Delta t$  and the wind Lorentz factor  $\Gamma$  are normalized in Eq. (2) to their typical values inferred from observations:  $L_\gamma = 10^{52}$  erg/s,  $E_\gamma^b = 1 E_{\gamma,\text{MeV}}^b$  MeV,  $\Delta t = 10^{-2}$  s, and  $\Gamma = 10^{2.5}$ . The proton break energy,  $E_p^b$ , is the threshold proton energy for interaction with photons of observed energy  $E_\gamma^b$ ,  $E_p^b = (2/E_{\gamma,\text{MeV}}^b) \Gamma_{2.5}^2 \times 10^7$  GeV.

The rate at which energy is produced as  $\gamma$ -rays by GRBs is similar to the rate of production of high energy,  $> 10^{19}$  eV, protons implied by the observed ultra-high energy cosmic-ray flux (Waxman 1995a,b,2000),

$$E_p^2 \frac{d\dot{n}_p}{dE_p} \approx 10^{44} \text{erg Mpc}^{-3} \text{yr}^{-1}. \quad (3)$$

Assuming that GRBs are the sources of observed ultra-high energy cosmic rays, the intensity of high energy muon neutrinos and anti-neutrinos implied by Eq. (2) is then (Waxman & Bahcall 1997,1999)

$$E_\nu^2 \Phi_\nu \approx 3 \times 10^{-9} \left[ \frac{f_\pi(E_p > E_p^b)}{0.2} \right] \min(1, E_\nu/E_\nu^b) \text{GeV/cm}^2 \text{sr s}. \quad (4)$$

Since neutrinos carry  $\approx 5\%$  of the proton energy, the neutrino break energy is given by

$$E_\nu^b \approx 10^{15} (1+z)^{-2} \frac{\Gamma_{2.5}^2}{E_{\gamma, \text{MeV}}^b} \text{eV}. \quad (5)$$

We have explicitly introduced here the dependence on source redshift,  $z$ , which is due to the fact that energies observed on Earth are smaller than those measured at the source redshift by a factor  $(1+z)$ .

The value of  $f_\pi$ , Eq. (2), is strongly dependent on  $\Gamma$ . It has recently been pointed out by Halzen and Hooper (1999) that if the Lorentz factor  $\Gamma$  varies significantly between bursts, with burst to burst variations  $\Delta\Gamma/\Gamma \sim 1$ , then the resulting neutrino flux will be dominated by a few neutrino bright bursts, and may significantly exceed the flux given by Eq. (4), derived for typical burst parameters. This may strongly enhance the detectability of GRB neutrinos by planned neutrino telescopes (Alvarez-Muniz, Halzen & Hooper 2000).

The main goal of the present work is to determine the allowed range of variation in the fraction of fireball energy converted to high energy neutrinos, under the assumption that GRBs are produced by internal dissipation shocks in an ultra-relativistic wind. We self-consistently calculate the dependence on wind parameters of both  $\gamma$ -ray emission by electrons and neutrino production by photo-meson interaction of protons, taking into account synchrotron losses of high energy pions and muons and pair-production interaction of high energy photons. We show that large burst-to-burst variations in the fraction of fireball energy converted to neutrinos are not expected, due to two reasons. First, the observational constraints imposed by  $\gamma$ -ray observations, in particular the requirement  $E_\gamma^b \geq 0.1$  MeV, imply that wind model parameters ( $\Gamma$ ,  $L$ ,  $\Delta t$ ) are correlated, and that  $\Gamma$  is restricted to values in a range much narrower than  $\Delta\Gamma/\Gamma \sim 1$ . Second, for wind parameters that imply, through Eq. (2),  $f_\pi$  values significantly exceeding 20%, only a small fraction of the pions' energy is converted to neutrinos due to pion and muon synchrotron losses.

The model we analyze is described in § 2. Numerical results are presented and discussed in § 3. Conclusions and implications are summarized in § 4.

## 2. OUTLINE OF THE MODEL

We consider a compact source, of linear scale  $R_0 \sim 10^6$  cm, which produces a wind characterized by an average luminosity  $L_w \sim 10^{52} \text{erg s}^{-1} - 10^{53} \text{erg s}^{-1}$  and mass loss rate  $\dot{M} = L_w / \eta c^2$  ( $R_0 \sim 10^6$  cm corresponds to three times the Schwarzschild radius of a non-rotating, solar mass black hole). At small radius, the wind bulk Lorentz factor,  $\Gamma$ , grows linearly with radius, until most of the wind energy is converted to kinetic energy and  $\Gamma$  saturates at  $\Gamma \sim \eta \sim 300$ .  $\eta \gtrsim 300$  is required to reduce the wind pair-production optical depth for observed high energy,  $> 100$  MeV, photons to less than unity. If  $\eta > \eta_* \approx (\sigma_T L_w / 4\pi m_p c^3 R_0)^{1/4} = 3 \times 10^3 (L_{w,53} / R_{0,6})^{1/4}$ , where  $L_w = 10^{53} L_{w,53} \text{erg s}^{-1}$  and  $R_0 = 10^6 R_{0,6}$  cm, the wind becomes optically thin at  $\Gamma \approx \eta_* < \eta$ , and hence acceleration saturates at  $\Gamma \approx \eta_*$  and the remaining wind internal energy escapes as thermal radiation at  $\sim 1$  MeV temperature. Variability of the source on time scale  $\Delta t$ , resulting in fluctuations in the wind bulk Lorentz factor  $\Gamma$  on similar time scale, leads to internal shocks in the expanding fireball at a radius  $R_i \approx 2\Gamma^2 c \Delta t = 6 \times 10^{13} \Gamma_{2.5}^2 \Delta t_{-2}$  cm. If the Lorentz factor variability within the wind is significant, internal shocks reconvert a substantial part of the kinetic energy to internal energy. It is assumed that this energy is then radiated as  $\gamma$ -rays by synchrotron (and inverse-Compton) emission of shock-accelerated electrons.

The dynamics of our model is described in § 2.1, and neutrino production calculations are described in § 2.2.

### 2.1. Model Dynamics

In this work, we use an approximate model of the unsteady wind described in the preceding paragraph, following Spada, Panaitescu & Mészáros 2000, and Guetta, Spada & Waxman 2000 (GSW00). The wind evolution is followed starting at radii larger than the saturation radius, i.e. after the shells have already reached their final Lorentz factor following the acceleration phase, and the GRB photon flux and spectrum resulting from a series of internal shocks that occur within the wind at larger radii are calculated.

The wind flow is approximated as a set of discrete shells. Each shell is characterized by four parameters: ejection time  $t_j$ , where the subscript  $j$  denotes the  $j$ -th shell, Lorentz factor  $\Gamma_j$ , mass  $M_j$ , and width  $\Delta_j$ . Since the wind duration,  $t_w \sim 10$  s, is much larger than the dynamical time of the source,  $t_d \sim R_0/c$ , variability of the wind on a wide range of time scales,  $t_d < t_v < t_w$ , is possible. For simplicity, we consider a case where the wind variability is characterized by a single time scale  $t_w > t_v > t_d$ , in addition to the dynamical time scale of the source  $t_d$  and to the wind duration  $t_w$ . Thus, we consider shells of initial thickness  $\Delta_j = ct_d = R_0$ , ejected from the source at an average rate  $t_v^{-1}$ .

In GSW00 we have examined the dependence of observed  $\gamma$ -ray flux and spectrum on wind model parameters, taking into account both synchrotron and inverse-Compton emission, and

the effect of  $e^\pm$  pair production. We have assumed there that the Lorentz factor of a given shell is independent of those of preceding shells, and considered various Lorentz factor distributions. We have shown that in order to obtain  $\gamma$ -ray flux and spectrum consistent with observations, large variance is required in wind Lorentz factor distribution. We therefore restrict the following discussion to the bimodal case, where Lorentz factors are drawn from a bimodal distribution,  $\Gamma_j = \Gamma_m$  or  $\Gamma_j = \Gamma_M \approx \eta_* \gg \Gamma_m$ , with equal probability. The time intervals  $t_{j+1} - t_j$  are drawn randomly from a uniform distribution with an average value of  $t_v$ . In GSW00 we have considered two qualitatively different scenarios for shell masses distribution, shells of either equal mass or equal energy, and concluded that observations favor shells of equal mass. We therefore restrict the following discussion to the equal shell mass case. We note, however, that our conclusions are not sensitive to this assumption.

Once shell parameters are determined, we calculate the radii where collisions occur and determine the photon and neutrino emission from each collision. In each collision a forward and a reverse shock are formed, propagating into forward and backward shells respectively. The plasma parameters behind each shock are determined by the Taub adiabat, requiring continuous energy density and velocity across the contact discontinuity separating the two shells (Panaitescu & Mészáros 1999). We assume that a fraction  $\epsilon_e$  ( $\epsilon_B$ ) of the protons shock thermal energy is converted to electrons (magnetic field). We assume that both electrons and protons are accelerated by the shocks to a power-law distribution,  $dn_\alpha/d\gamma_\alpha \propto \gamma_\alpha^{-p}$  for particle Lorentz factors  $\gamma_{\alpha,\min} < \gamma_\alpha < \gamma_{\alpha,\max}$ . The maximum Lorentz factor is determined by equating the acceleration time, estimated as the Larmor radius divided by  $c$ , to the minimum of the dynamical time and the synchrotron cooling time.

The calculation of emitted  $\gamma$ -ray spectrum and flux is carried according to the method described in detail in GSW00, taking into account both synchrotron and inverse Compton emission, as well as the effect of the optical thickness due to Thomson scattering on both electrons present initially in the flow and those created by pair production. Here we focus on neutrino production by photo-meson interactions, following Waxman & Bahcall 1997. Our method of calculation is described below.

## 2.2. Neutrino production

The fraction  $f_\pi(E_p)$  of proton energy lost to pion production is estimated as  $f_\pi = \min(1, \Delta t/t_\pi)$  where  $\Delta t$  is the comoving shell expansion time and  $t_\pi$  is the proton photo-pion energy loss time (Waxman & Bahcall 1997),

$$\begin{aligned} t_\pi^{-1}(E_p) &= -\frac{1}{E_p} \frac{dE_p}{dt} \\ &= \frac{1}{2\gamma_p^2} c \int dE \sigma_\pi(E) \xi(E) E \int_{E/2\gamma_p}^{\infty} dx x^{-2} n(x). \end{aligned} \quad (6)$$

Here  $\sigma_\pi(E)$  is the cross section for the pion production for a photon with energy  $E$  in the proton rest frame,  $\xi(E)$  is the average fraction of energy lost to the pion, and  $n(E)$  is the comoving number density of photons per unit energy. In our calculations, we have approximated the integral, Eq. (6), by the contribution from the  $\Delta$  resonance. This approximation is valid for GRB photon spectra (Waxman 2000).

Photo-meson production of low energy protons, well below  $E_p^b$ , requires interaction with high energy photons, well above  $E_\gamma^b$ . Such photons may be depleted by pair production. For each collision we find the photon energy  $E_\gamma^\pm$ , for which the pair production optical thickness,  $\tau_{\gamma\gamma}$ , is unity. A large fraction of photons of energy exceeding  $\max(E_\gamma^\pm, m_e c^2)$  (measured in the shell frame) will be converted to pairs, and hence will not be available for photo-meson interaction, leading to a suppression of the neutrino flux at low energies. In order to take this effect into account, we use  $f_\pi = \min[1, (\Delta t/t_\pi) \min(1, \tau_{\gamma\gamma}^{-1})]$  for protons interacting with photons which are strongly suppressed by pair production.

Neutrino production is suppressed at high energy, where neutrinos are produced by the decay of muons and pions whose lifetime  $\tau$  exceeds the characteristic time for energy loss due to synchrotron emission (Waxman & Bahcall 1997, 1999, Rachen & Mészáros 1998). We therefore define an effective  $f_\pi$ ,  $f_{\pi,\text{eff.}}$ , as  $4f_\pi$  times the fraction of pions' energy converted to muon neutrinos. In the absence of pion and muon energy loss,  $\approx 1/4$  of the pions' energy is converted to muon neutrinos, since  $\approx 1/2$  the energy of charged pions is converted to  $\nu_\mu + \bar{\nu}_\mu$ . Thus,  $f_{\pi,\text{eff.}}$  is the fraction of proton energy that, in the absence of synchrotron losses, leads to approximately the same muon neutrino flux as that obtained when synchrotron losses are taken into account.

In each collision a fraction of the kinetic energy of the colliding shell is converted to a flux of photons and neutrinos. The energy that is not lost to photons and neutrinos is converted back to kinetic energy by adiabatic expansion of the shell.

### 3. RESULTS AND DISCUSSION

In this section we determine the dependence of  $f_{\pi,\text{eff.}}$ , the fraction of proton energy that in the absence of synchrotron losses leads to approximately the same muon neutrino flux as that obtained when synchrotron losses are taken into account, on wind model parameters. We adopt electron and magnetic field energy fractions close to equipartition,  $\epsilon_e = 0.45$  and  $\epsilon_B \geq 0.01$ , and  $p = 2$ . The equipartition fractions are required to satisfy  $\epsilon_e \geq 0.1$  and  $\epsilon_B \geq 0.01$  in order to account for observed  $\gamma$ -ray emission (e.g. GSW00). Moreover,  $\epsilon_e$  values in the range of 0.1 to 0.5 are typically derived from GRB afterglow observations (e.g. Freedman & Waxman 2001).  $p \simeq 2$  is required to account for observed  $\gamma$ -ray and afterglow spectra (Freedman & Waxman 2001). Figure 1 presents contour plots of the photon break energy,  $E_\gamma^b$ , as function of  $\Gamma_m$  and  $t_v$  for  $L_w = 10^{53}$  erg/s and and  $\epsilon_B = 0.01$ ,  $\epsilon_B = 0.1$ . The qualitative behavior demonstrated by the contour plot can be understood based on the following arguments. The wind energy density at the smallest radii of

the internal dissipation shocks is lower for higher values of  $\Gamma_m$ , leading to a decrease of  $E_\gamma^b$  with increasing  $\Gamma_m$ . This effect sets the upper bound on  $\Gamma_m$  values. Lowering the value of  $\Gamma_m$  leads to increase in  $E_\gamma^b$  together with increase in the wind optical depth at the smallest internal shocks radii. Once the optical depth exceeds unity, emission is strongly suppressed leading to a rapid decrease with  $\Gamma_m$  of both the fraction of wind energy escaping as radiation and  $E_\gamma^b$  (see GSW00 for detailed discussion).

Figure 2 presents the contour plot for the effective  $f_\pi$ ,  $f_{\pi,\text{eff}}$ , for the case shown in Figure 1 with  $\epsilon_B = 0.01$ . The values shown are averaged over all internal collisions, weighted by the energy converted to high energy protons in each collision. Values of  $f_\pi$  are shown for several neutrino energy ranges, using the approximation  $E_\nu = 0.05E_p$ . The region in  $\Gamma_m$ - $t_v$  plane where  $E_\gamma^b > 0.1$  MeV is bound in Figure 2 by the dashed line. The dash-dotted line outlines the region in which the fraction of wind energy converted to radiation exceeds 2% (higher fraction is obtained for larger  $\Gamma_m$  values). For wind parameters consistent with observed GRB characteristics, the effective value of  $f_\pi$  at high neutrino energy,  $E_\nu > E_\nu^b$ , is restricted to values in the range of  $\approx 10\%$  to  $\approx 30\%$ . Figure 3 presents the fraction  $f_\nu^{\text{thin}}$  of the fireball neutrino flux produced by internal shocks which are optically thin to radiation. While at high energy most of the neutrino flux is produced in the optically thin regime, where collisions also contribute to the photon flux, a large fraction,  $\sim 50\%$ , of the neutrino flux at low energy is produced by collisions which do not contribute to the observed gamma-ray flux. The optically thick collisions provide a significant contribution only at low energy, since the large energy density at these collisions lead to strong suppression of high energy neutrino production by muon and pion synchrotron losses.

In figure 4 we present contour plots of  $f_\pi$ , neglecting the effects on neutrino production of synchrotron losses and pair-production.  $f_\pi$  approaches unity at low values of  $\Gamma_m$  for low proton (neutrino) energy, and at intermediate values of  $\Gamma_m$  for high proton (neutrino) energy. The energy loss of pions and muons due to synchrotron emission reduces the fraction of pion energy converted to neutrinos, and hence suppresses the effective value of  $f_\pi$ , to the range of values shown in Figure 2. The suppression seen in Figure 4 of  $f_\pi$  at low  $\Gamma_m$  for high energy protons is due to the fact that for low values of  $\Gamma_m$  most collisions occur at small radii, where synchrotron losses of high energy protons prevent acceleration of protons to ultra-high energy (Waxman 1995a). Ultra-high energy protons are produced in this case only at secondary collisions at large radii, where the photon energy density is already low, resulting in smaller values of  $f_\pi$ .

Figures 5 and 6 present  $f_{\pi,\text{eff}}$  for  $L_w = 10^{53}$  erg/s,  $\epsilon_B = 0.1$  and  $L_w = 10^{52}$  erg/s  $\epsilon_B = 0.01$  respectively. Comparing to the results presented in Figure 2, we find that the qualitative behavior as well as the predicted values of  $f_{\pi,\text{eff}}$  are not sensitive to wind luminosity and magnetic field equipartition fraction (over the range allowed by GRB observations).

The neutrino break energy inferred from Figures 2, 5 and 6,  $E_\nu^b \sim 10^{15}$  eV, is somewhat higher than estimated by Waxman & Bahcall (1997),  $E_\nu^b \sim 10^{14}$  eV [see Eq. (5)], since the photon energy break in our wind models is typically  $E_\gamma^b \sim 0.1$  MeV, rather than  $E_\gamma^b \sim 0.5$  MeV. Note, that

although synchrotron losses suppress neutrino production at high energy (compare Figures 2 and 4), the increase in  $f_\pi$  at high energy (Figure 2) implies that the neutrino flux is flat, with roughly equal energy per logarithmic neutrino energy interval above  $E_\nu^b$ , in contrast with the expectation of strong suppression of neutrino flux at  $E_\nu \gtrsim 10^{16}$  eV (Waxman & Bahcall 1997, 1999, Rachen & Mészáros 1998). This is due to two effects. First, high energy protons and neutrinos are produced in the present model over a very wide range of radii, over part of which synchrotron losses are small. Second, the low energy,  $E_\gamma < E_\gamma^b$ , photon spectrum obtained in the present model,  $E_\gamma^2(dn_\gamma/dE_\gamma) \propto E_\gamma^{1/2}$ , is softer than assumed in previous analyses,  $E_\gamma^2(dn_\gamma/dE_\gamma) \propto E_\gamma^1$ . GRB observation suggest that the latter, harder, spectrum is closer to reality, and steepening of the spectrum at low photon energy is indeed expected due to effects not included in the present analysis, such as inverse-Compton suppression and photospheric emission (see GSW00 for discussion). Thus, the present analysis most likely overestimates the value of  $f_{\pi,\text{eff.}}$  for  $E_\nu \gg E_\nu^b$ .

#### 4. CONCLUSIONS

We have studied neutrino production in GRBs, within the framework of the dissipative fireball model. We have considered photo-meson production of neutrinos in internal dissipation shocks by interaction of accelerated protons with observed  $\gamma$ -rays, taking into account synchrotron losses of high energy pions and muons and pair-production interaction of high energy photons. Our main results are presented in Figures 2, 5 and 6, showing the dependence on fireball wind model parameters of  $f_{\pi,\text{eff.}}$ , the fraction of proton energy that in the absence of synchrotron losses leads to approximately the same muon neutrino flux as that obtained when synchrotron losses are taken into account ( $f_{\pi,\text{eff.}}$  is defined as  $4f_\pi$  times the fraction of pions' energy converted to muon neutrinos). Over the range of wind model parameters, which produce photon break energy consistent with observations (bounded by the dashed line in the figures), the value of  $f_{\pi,\text{eff.}}$  at high neutrino energy,  $E_\nu > E_\nu^b$ , is within the range of  $\approx 10\%$  to  $\approx 30\%$ . The weak dependence of  $f_{\pi,\text{eff.}}$  on wind model parameters, in contrast with the strong dependence implied by Eq. (2), is due to two reasons. First, for low values of  $\Gamma$  and  $\Delta t$ , where large values of  $f_\pi$  are implied by Eq. (2), only a small fraction of the pions' energy is converted to neutrinos at high proton energy due to pion and muon synchrotron losses (compare figures 2 and 4). Second, the observational constraints imposed by  $\gamma$ -ray observations imply that wind model parameters ( $\Gamma$ ,  $L$ ,  $\Delta t$ ) are correlated.

Our results imply that GRB neutrino flux of individual bursts should correlate mainly with the bursts'  $\gamma$ -ray flux. An estimate of the time averaged neutrino intensity produced by GRBs may be obtained as follows. The average GRB fluence over the energy range observed by BATSE,  $\sim 0.1$  MeV to  $\sim 2$  MeV, is  $1.2 \times 10^{-5}$  eV. This corresponds to an average  $\gamma$ -ray intensity of  $E_\gamma^2 \Phi_\gamma \approx 0.8 \times 10^{-8}$  GeV/s sr cm<sup>2</sup>. The energy emitted as  $\gamma$ -rays is the energy converted to high energy electrons in internal fireball shocks which are optically thin to  $\gamma$ -rays (the electron synchrotron cooling time is short compared to the wind dynamical time). Denoting the fraction of thermal proton energy converted to electrons in internal shocks by  $\epsilon_e$ , the expected muon neutrino

intensity is

$$E_\nu^2 \Phi_\nu \approx \frac{1}{4} \frac{f_{\pi,\text{eff.}}^{\text{thin}} (1 - \epsilon_e)}{f_\nu^{\text{thin}} \epsilon_e} 2E_\gamma^2 \Phi_\gamma \approx 2 \frac{f_{\pi,\text{eff.}}^{\text{thin}} (1 - \epsilon_e)}{0.2 f_\nu^{\text{thin}} 2\epsilon_e} \times 10^{-9} \text{GeV/s sr cm}^2, \quad (7)$$

where  $f_{\pi,\text{eff.}}^{\text{thin}}$  is the value of  $f_{\pi,\text{eff.}}$  averaged over optically thin collisions only, and  $f_\nu^{\text{thin}}$  is the fraction of the neutrino flux produced by optically thin collisions (the factor of 2 is due to the fact that the electron energy over a logarithmic energy interval is twice that of the photon energy per logarithmic photon energy interval). As discussed in §3, the contribution of optically thick collisions to neutrino flux is significant only at low energies, see Figure 3. Thus, the ratio  $f_{\pi,\text{eff.}}^{\text{thin}}/f_\nu^{\text{thin}}$  presented in Figure 7 is similar to  $f_{\pi,\text{eff.}}$  (Figure 2), except at low energy, where it exceeds  $f_{\pi,\text{eff.}}$  by a factor of  $\approx 2$ .

For  $\epsilon_e$  values implied by observations, typically  $0.1 \lesssim \epsilon_e \lesssim 0.5$ , the neutrino intensity given by Eq. (7), which is based on the observed intensity of GRB  $\gamma$ -ray photons, is similar to that given by Eq. (4) derived based on the assumption that GRBs are the sources of ultra-high energy cosmic-rays. This similarity reflects the fact that the  $\gamma$ -ray energy generation rate of GRBs is similar to the generation rate of high energy protons required to account for the observed flux of ultra-high energy cosmic-rays. Note, that we have used many simplifying assumptions in our analysis of the variable fireball wind (see § 2). Hence, the numerical values derived by our approximate analysis should not be considered more accurate than the estimates given by Eqs. (2,7). Nevertheless, the qualitative conclusions regarding the role of synchrotron and pair-production suppression and regarding the weak dependence of  $f_{\pi,\text{eff.}}$  on wind model parameters are not sensitive to the details of the approximations we have used, and are therefore of general validity. We note, in particular, that the value of  $f_{\pi,\text{eff.}}$  does not significantly exceed 20% also in wind model parameter regions which are outside the parameter region implied by observations.

Finally, we would like to make the following point. Fireball winds with Lorentz factors below the range allowed by observations produce low photon luminosity bursts, with characteristic photon energies well below 100 keV (see GSW00). While such bursts may not be detected by present photon detectors, and hence we currently have no evidence for their existence, they may contribute to the background neutrino intensity. Constraints on the high energy neutrino intensity may therefore provide constraints on the existence of such non-GRB fireballs.

The research of DG and MS is supported by COFIN-99-02-02. EW is partially supported by BSF Grant 9800343, AEC Grant 38/99 and MINERVA Grant. D.G. and M.S. thank the Weizmann Institute of Science, where part of this research was carried out, for the hospitality and for the pleasant working atmosphere.

## REFERENCES

- Alvarez-Muniz, J., Halzen, F. 2000, & Hooper, D. W., Phys. Rev. **D62**, 093015.
- Bahcall, J. N., & Mészáros, P. 2000, Phys. Rev. Lett. **85**, 1362.
- Fishman, G. J. & Meegan, C. A. 1995, ARA&A **33**, 415.
- Freedman, D. L., & Waxman, E. 2001, Ap. J. **547**, 922.
- Guetta, Spada & Waxman, astro-ph/0011170, submitted to apJ (GSW00).
- Halzen, F. & Hooper, D. W. 1999, ApJ, 527, L93.
- Kulkarni, S. R. *et al.*, To appear in Proc. of the 5th Huntsville Gamma-Ray Burst Symposium (astro-ph/0002168).
- Mészáros, P. 1999, A&AS **138**, 533.
- Mészáros, P., & Rees, M. 2000, Ap. J. **541**, L5.
- Panaitescu, A., Spada, M. & Mészáros, P. 1999, **526**, 707.
- Piran, T. 1999, Phys. Rep. **314**, 575.
- Rachen P. & Mészáros P. 1998, Phys. Rev. **D 58**, 123005.
- Spada, M., Panaitescu, A., & Mészáros, P. 2000, Apj, **537**, 824.
- Vietri, M. 1995, Ap. J. **453**, 883.
- Waxman, E. 1995, Phys. Rev. Lett. **75**, 386.
- Waxman, E. 1995, Ap. J. **452**, L1.
- Waxman, E. 2000, Nucl. Phys. B (Proc. Suppl.) **87**, 345.
- Waxman, E., & Bahcall 1997, J. N., Phys. Rev. Lett. **78**, 2292.
- Waxman, E., & Bahcall 1999, J. N., Phys. Rev. **D59**, 023002.
- Waxman, E., & Bahcall 2000, J. N., Ap. J. **541**, 707.

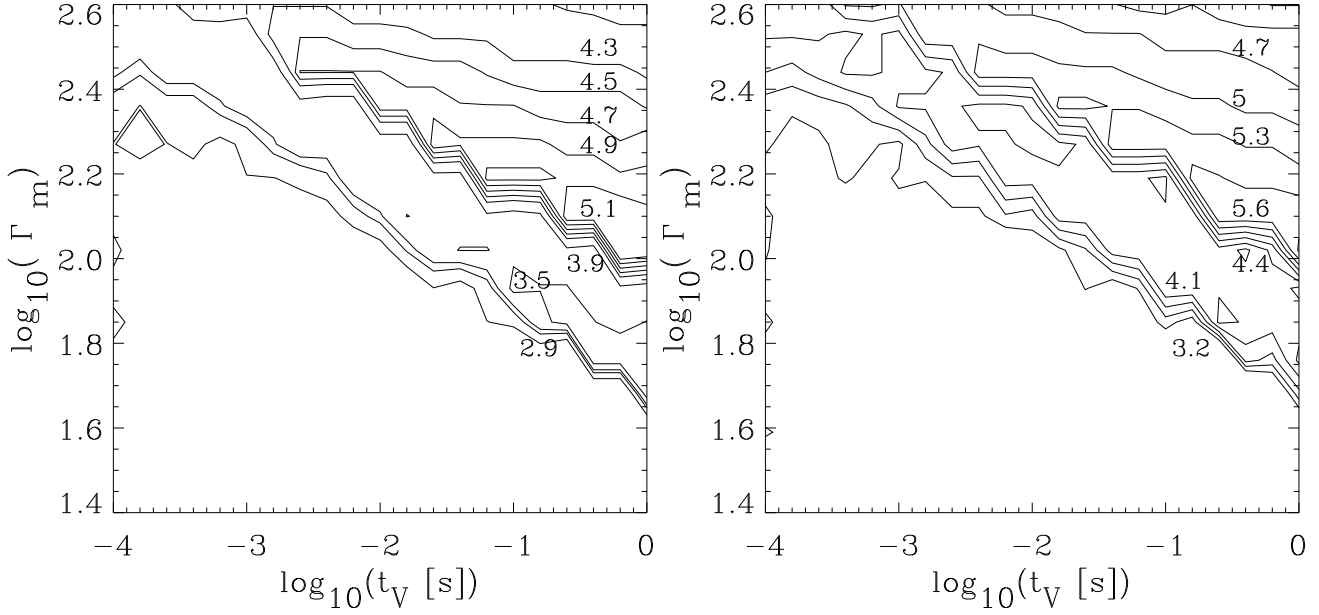


Fig. 1.— Contour plots of observed photon spectral break energy (where photon luminosity per logarithmic photon energy interval peaks),  $\log_{10}(E_\gamma^b[\text{eV}])$  as function of wind variability time  $t_v$  and minimum Lorentz factor  $\Gamma_m$ , for  $L_w = 10^{53}\text{erg/s}$  and  $\epsilon_B = 0.01$  (left panel),  $\epsilon_B = 0.1$  (right panel). The wind maximum Lorentz factor is  $\Gamma_M = 2500$ , and the source is assumed to lie at  $z = 1.5$ .

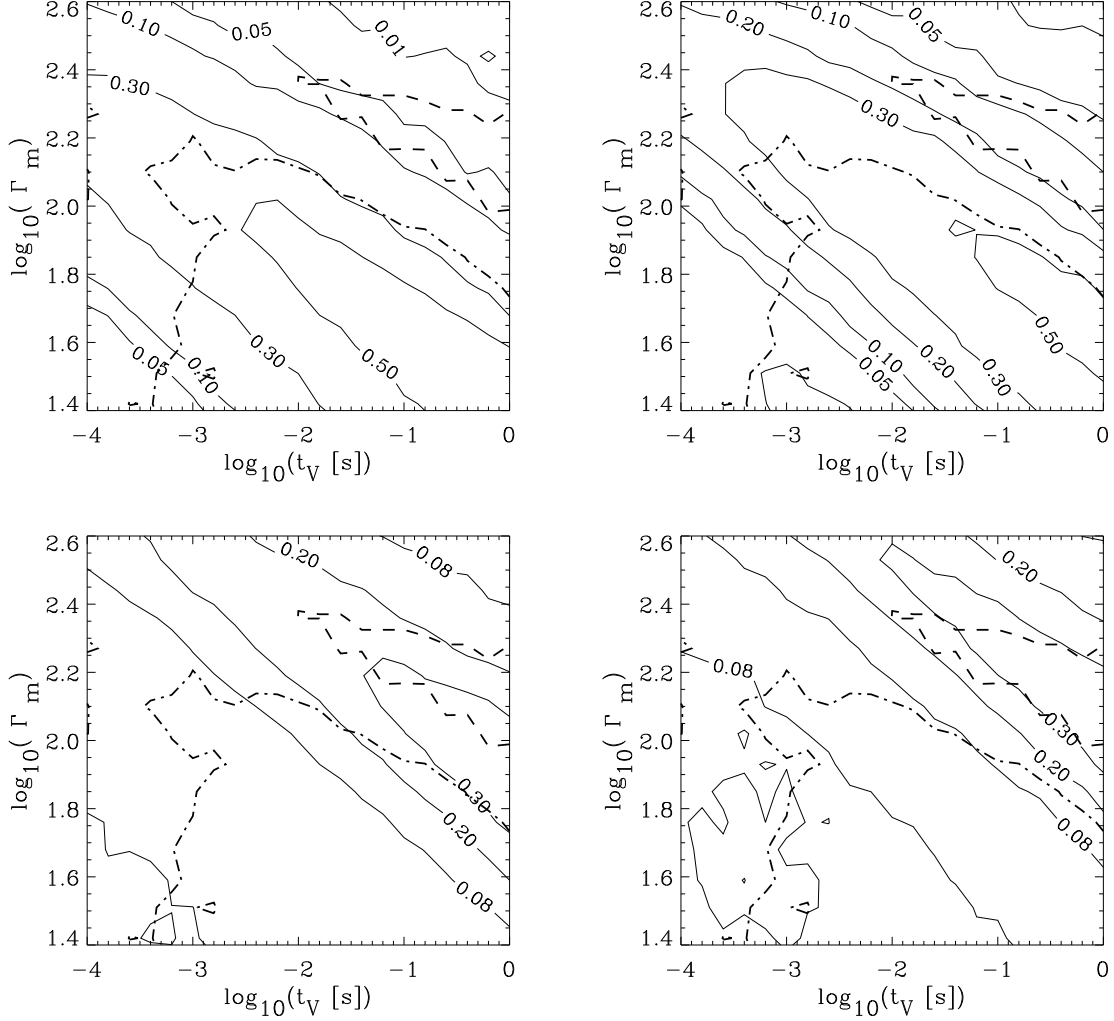


Fig. 2.— Contour plots of  $f_{\pi, \text{eff}}$ , the effective value of  $f_\pi$  (defined as  $4f_\pi$  times the fraction of pions’ energy converted to muon neutrinos), as function of wind variability time  $t_v$  and minimum Lorentz factor  $\Gamma_m$ , for wind luminosity  $L_w = 10^{53} \text{ erg/s}$  and  $\epsilon_B = 0.01$ . The four panels correspond to four observed neutrino energy bins, clockwise from top left:  $10^{14} \text{ eV} < E_\nu < 10^{15} \text{ eV}$ ,  $10^{15} \text{ eV} < E_\nu < 10^{16} \text{ eV}$ ,  $10^{17} \text{ eV} < E_\nu < 10^{18} \text{ eV}$ ,  $10^{18} \text{ eV} < E_\nu < 10^{19} \text{ eV}$ . We have used the approximate relation  $E_\nu = 0.05 E_p$  between neutrino and proton energy, and assumed a source redshift  $z = 1.5$ . The region in  $\Gamma_m$ - $t_v$  plane where  $E_\gamma^b > 0.1 \text{ MeV}$  is bound by the dashed lines. The dash-dotted lines outline the region in which the fraction of wind energy converted to radiation exceeds 2% (higher fraction is obtained at larger  $\Gamma_m$  values).

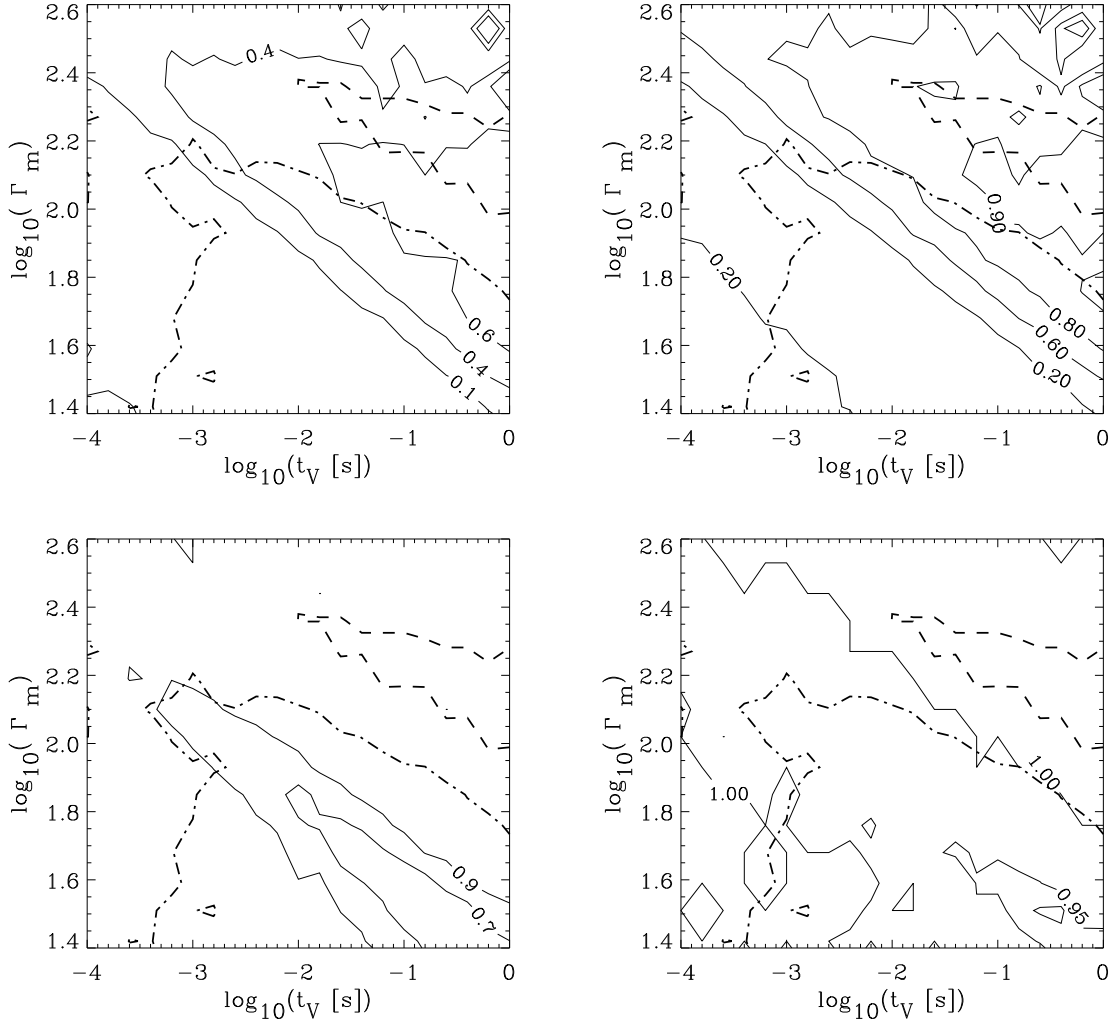


Fig. 3.— Contour plots of  $f_\nu^{\text{thin}}$ , the fraction of the neutrino flux produced by optically thin collisions, as function of wind variability time  $t_v$  and minimum Lorentz factor  $\Gamma_m$ , for the case shown in Figure 2.

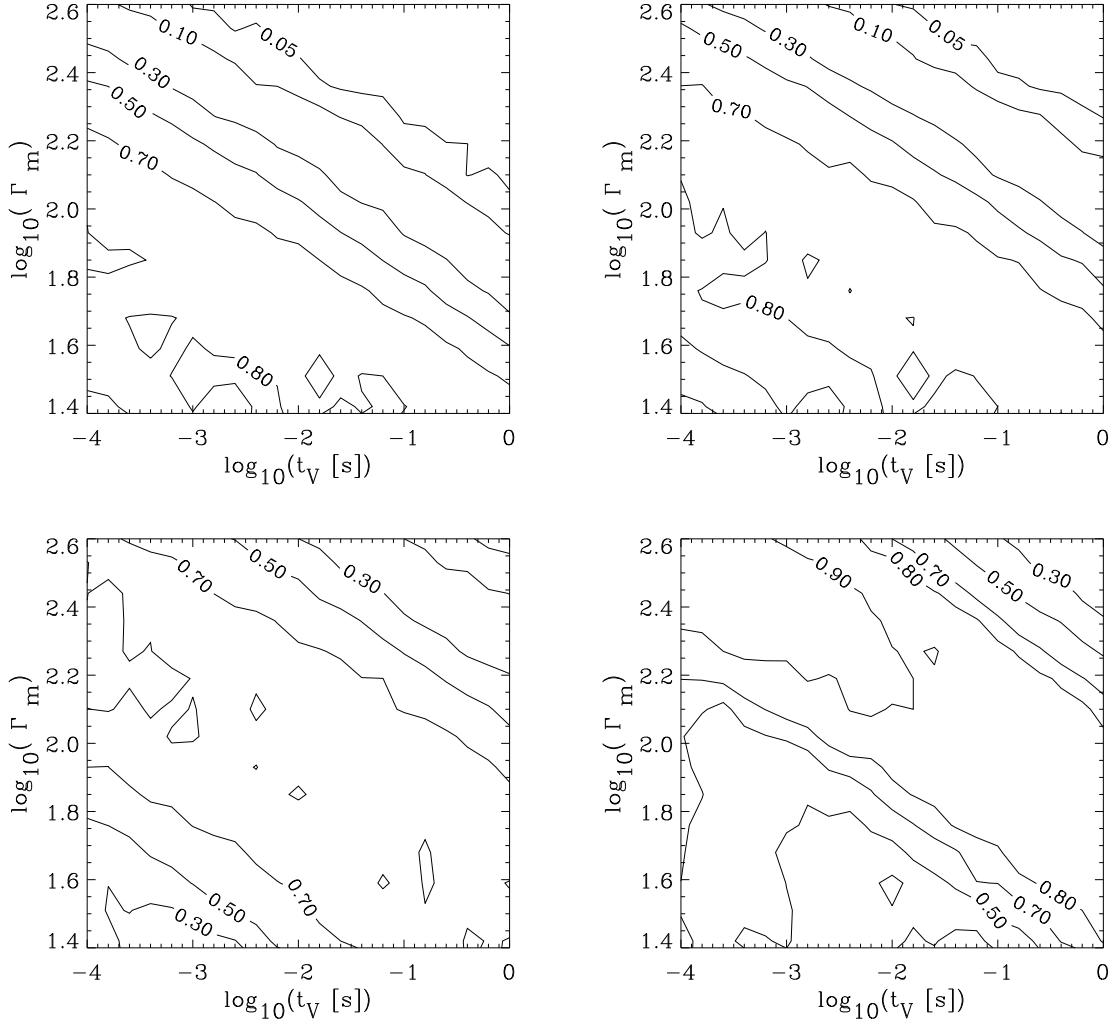


Fig. 4.— Contour plots of  $f_\pi$ , obtained when the effects on neutrino production of synchrotron losses and pair-production are neglected, for the case shown in Figure 2.

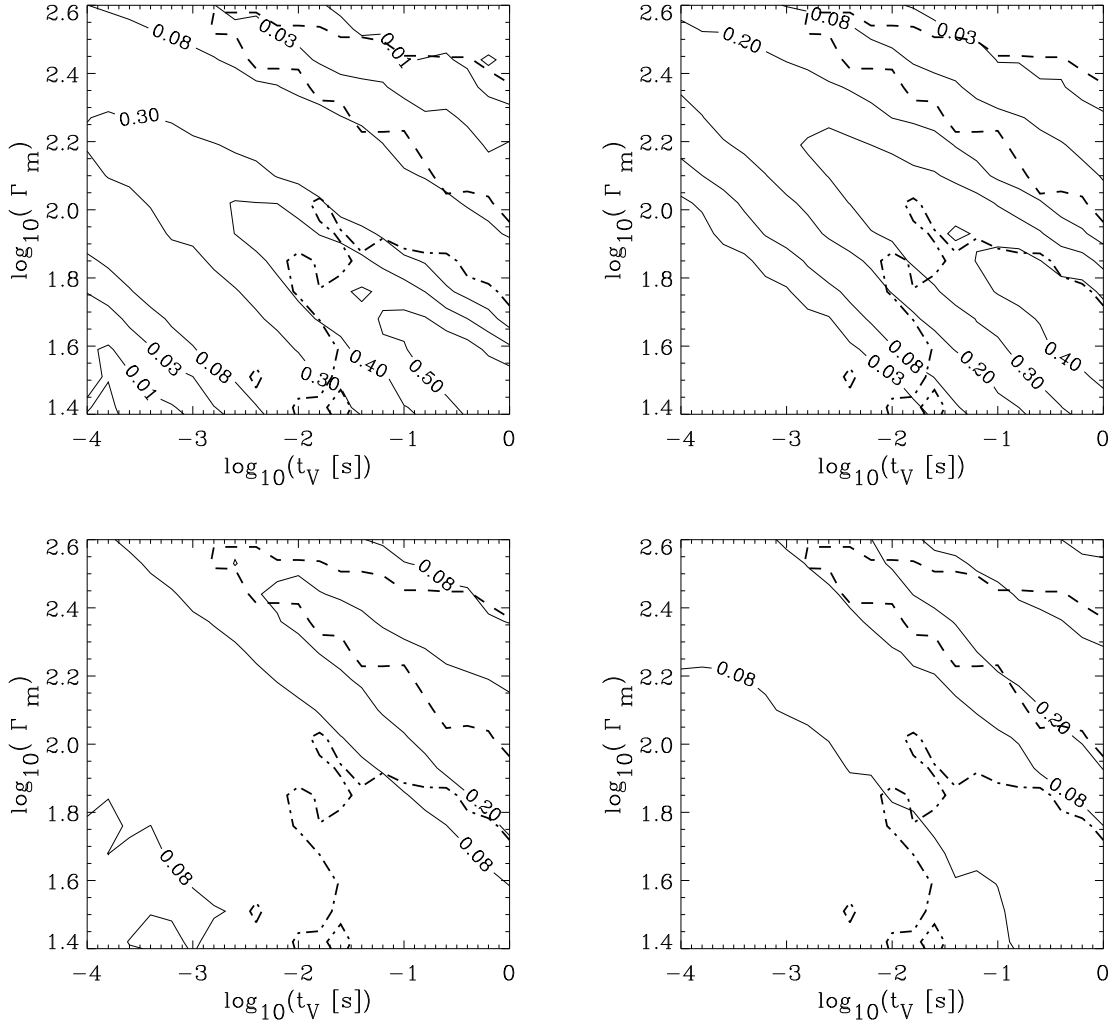


Fig. 5.— Same as Fig.2, for different equipartition parameter  $\epsilon_B = 0.1$ .

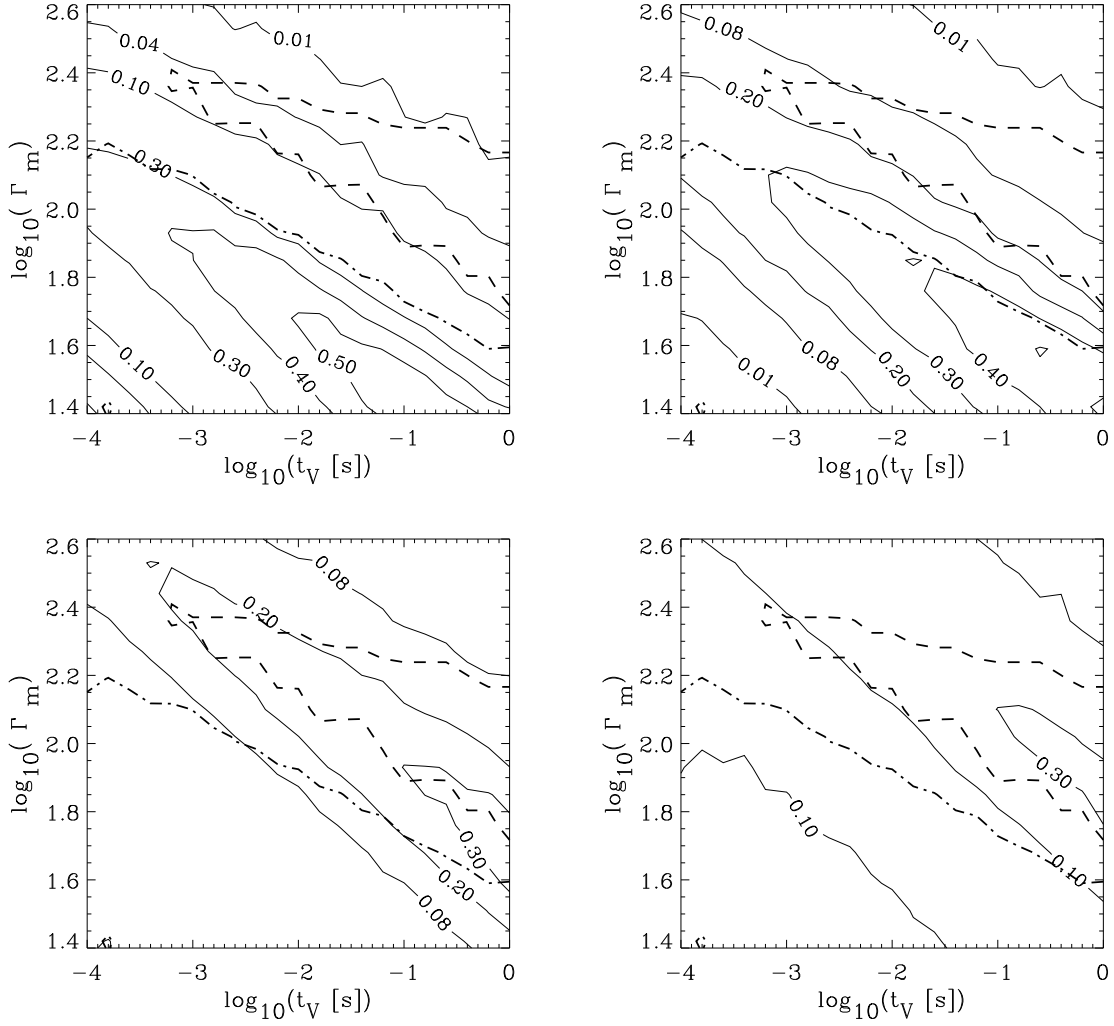


Fig. 6.— Same as Fig.2, for different luminosity  $L_w = 10^{52}$ erg/s.

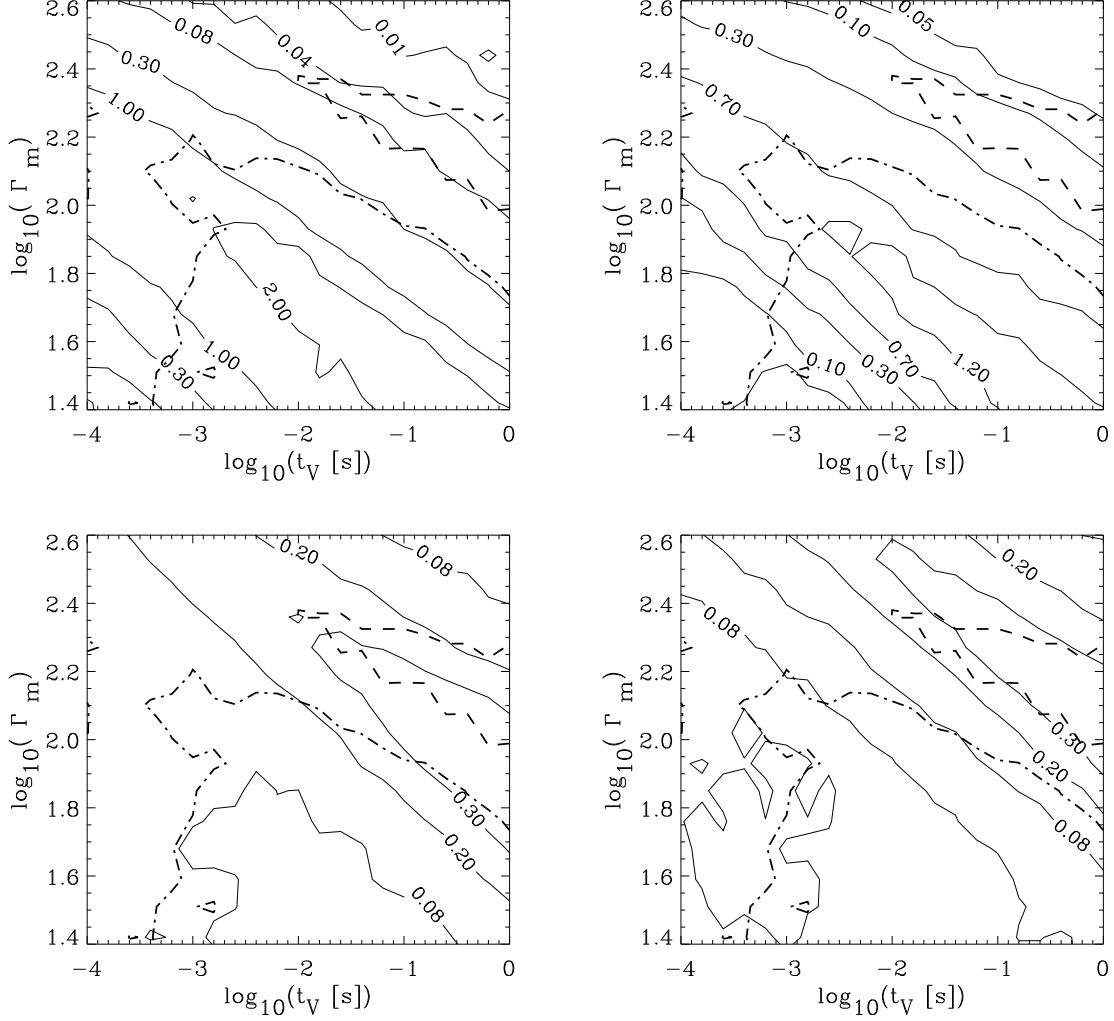


Fig. 7.— Contour plots of the ratio  $f_{\pi,eff}^{thin}/f_{\nu}^{thin}$ , as function of wind variability time  $t_v$  and minimum Lorentz factor  $\Gamma_m$ , for the case shown in Figure 2.  $f_{\pi,eff}^{thin}$  is the value of  $f_{\pi,eff}$  averaged over optically thin collisions only and  $f_{\nu}^{thin}$ , the fraction of the neutrino flux produced by optically thin collisions, is shown in Fig. 3.